Effects of dissolved oxygen and ion irradiation on the corrosion of FeCrAl-ODS in high-temperature water simulating BWR operating conditions

T. SATO, Y. NAKAHARA, F. UENO, S. YAMASHITA
Japan Atomic Energy Agency
2-4 Shirakata Shirane, Tokai-mura, Naka-gun, Ibaraki-ken 319-1195, Japan

K. SAKAMOTO
Nippon Nuclear Fuel Development, Co., Ltd.
2163 Narita-cho, Oarai-machi, Ibaraki-ken, 311-1313 – Japan

ABSTRACT

This study aims to investigate the applicability of FeCrAl-based and oxide-dispersion-strengthened alloys (FeCrAl-ODS) to fuel cladding of accident tolerant fuel (ATF) for boiling water reactors (BWRs). Corrosion property of the FeCrAl-ODS plays an important role in the BWR conditions.

In this study, *in-situ* electrochemical impedance spectrometry (EIS) was conducted to investigate the effects of dissolved oxygen (DO) and irradiation on the corrosion of FeCrAl-ODS in high-temperature water simulating BWR operation conditions. The specimens were irradiated with a beam of iron ions in the air. Based on results obtained in this study, the following conclusions were drawn:

(1) The modulus of impedance initially increased with time, and then became stable. In this study, the time required to reach stabilization increased with a decrease in DO.
(2) The estimated corrosion depth of FeCrAl-ODS in deaerated condition was less than 3 μm, which was the deepest value found in this study.
(3) There was a little difference between the modulus of the impedance responses of the irradiated FeCrAl-ODS specimens and that of the non-irradiated specimens, which indicated that radiation damage to FeCrAl-ODS might not affect its corrosion properties in high-temperature water.

1. Introduction

The applicability of FeCrAl-based and oxide-dispersion-strengthened alloys (FeCrAl-ODS) to the fuel cladding of accident tolerant fuel (ATF) for boiling water reactors (BWRs) was investigated in Japan. One of the important properties of FeCrAl-ODS in BWR conditions is its corrosion property.

Water radiolysis occurs around fuel assemblies and hydrogen peroxide generated. The generated hydrogen peroxide is an oxidant and it shifts the electrochemical corrosion potential of stainless steel nobler. To simulate the nobler potential conditions, corrosion and stress corrosion cracking (SCC) tests were conducted in high-temperature water with a high concentration of oxygen (8ppm) to evaluate irradiation assisted SCC. One countermeasure that was used to neutralize the effects of the water radiolysis in reactor coolant was the injection of hydrogen into the coolant. The injected hydrogen recombined with oxygen and hydrogen peroxide to form water. To apply the FeCrAl-ODS in BWRs, understanding the effects of dissolved oxygen (DO) on the corrosion behavior of FeCrAl-ODS is important.

The fuel cladding is exposed to strong irradiation in the core, which causes damage to the FeCrAl-ODS. However, few studies have reported data on the effects of irradiation on the corrosion of FeCrAl-ODS in high-temperature water.

In this study, *in-situ* electrochemical impedance spectrometry (EIS) was used to investigate the effects of DO and irradiation on the corrosion of FeCrAl-ODS in high-temperature water user simulated BWR conditions.

2. Experiment

2.1 Electrochemical test equipment

A schematic diagram of the high temperature water loop is shown in Fig. 1 [1,2]. The water flowed from the makeup water tank to the autoclave. The concentration of DO was controlled by bubbling nitrogen and oxygen gasses in the makeup water tank. First, water flowed out from the autoclave, it was then cooled and cleaned using the ion exchange resin, and sent back to the makeup water tank. The DO concentration and conductivity of the inlet water were continuously monitored.

Plate-type test specimens of FeCrAl-ODS were installed in the autoclave. A high temperature was maintained inside the autoclave to simulate BWR operating conditions. Images of the installed test specimens are shown in Fig. 2. The size of the test specimen was 10 x 10 x 1 mm^t. Two specimens made of the same material were placed in the autoclave at the same time to measure their respective EIS values. The corners of the specimens were thinned so that they could be set in a holder for iron ion beam irradiation. To evaluate the effects of irradiation, 3 sets of test specimens with different irradiation conditions were placed in the autoclave at the same time, as shown in Fig.3.

A sine wave voltage was applied between the test specimens to measure EIS. The voltage was 30 mV_{p-p} and the frequency was varied between 100 Hz and 1 mHz.

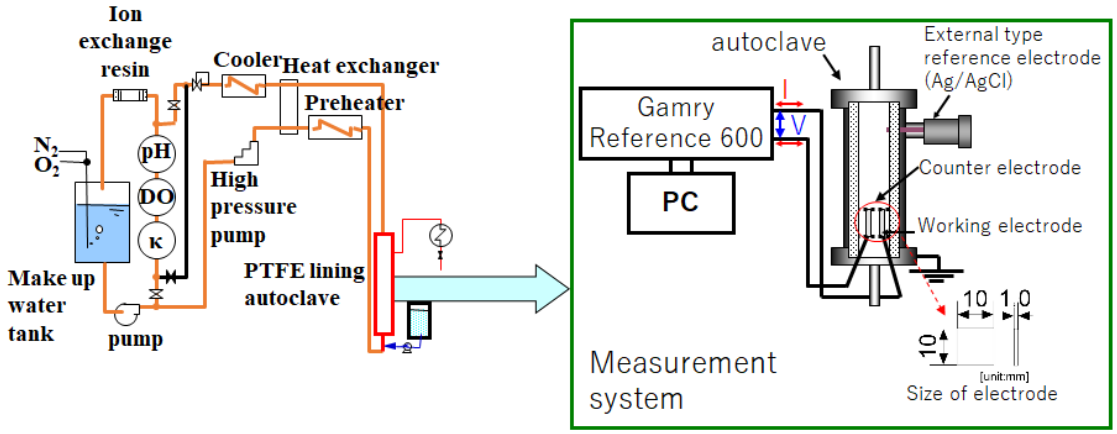

Fig. 1 A schematic diagram of the high temperature high pressure water loop

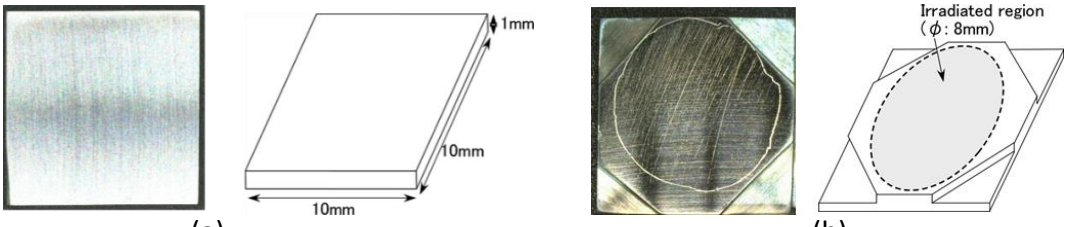

(a) (b)

Fig. 2 Test specimens ((a): for the test of DO effect and, (b): for the test of irradiation effect)

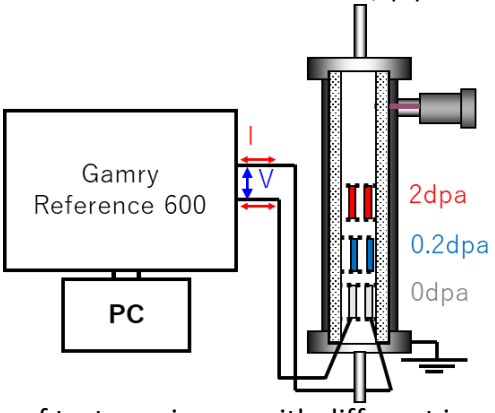

Fig. 3 A schematic view of test specimens with different irradiation conditions in the

autoclave

2.2 Corrosion test and irradiation conditions

The experimental conditions of the corrosion test and irradiation variations are listed in Table 1. The temperature simulated BWR conditions, DO concentration was a valuable parameter, iron ions beam was selected, and the irradiation dose was also a valuable parameter. The ion irradiation was performed at the Takasaki Ion Accelerators for Advanced Radiation Application (QST TIARA) facility. An example of the calculated depth profile of the irradiation damage by SRIM are shown in Fig. 4. The irradiation damage at the surface was about 1/3 of that at 1μm.

Experimental conditions	
Corrosion test conditions	
Temperature	280 °C
Pressure	8.5 MPa
Dissolved O_2	<0.005, 0.25, 8ppm
Conductivity	<0.06 uS/cm
Surface treatment	#800 mechanical polished
Ion irradiation conditions	
Dose rate	$1.6x10^{-4}$ dpa/s at 1 um
Total dose	0dpa, 0.2dpa, 2dpa at 1 um
Kind of beam	Iron ions beam
Irradiation temp.	300 °C
Energy of ions	10.5MeV
Irradiation current	< 0.2uA

Table 1 List of experimental conditions

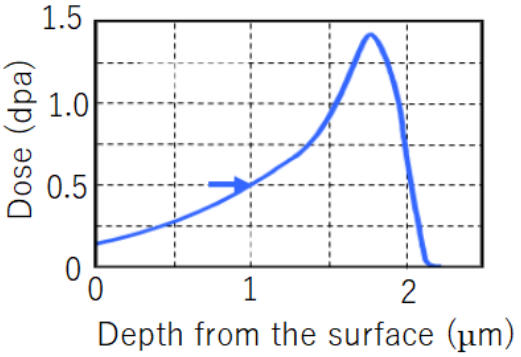

Fig. 4. Depth profile of irradiation damage

3. Results and Discussion

3.1 Effects of dissolved oxygen concentration

The dependency of impedance response of FeCrAl-ODS on the DO concentration was investigated. Nyquist plots of the experimentally-obtained impedances are shown in Fig. 5. The horizontal axis and vertical axis represent the real and imaginary part of the impedance, respectively. Half circles were obtained, and it was found that their diameter when the DO was 8 ppm was larger than that when it was 0.25 ppm. The impedance response in the lower frequency range can be determined by the polarization resistance. The larger diameters of the half circles were indicative of the higher polarization resistance at the surface of FeCrAl-ODS.

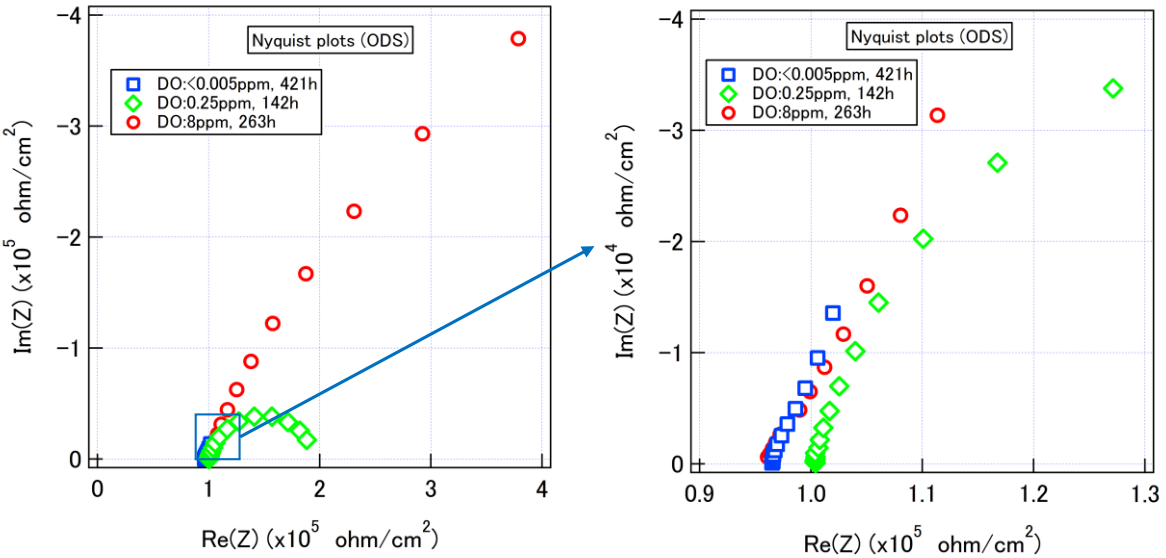

Fig. 5 The Nyquist plots of the obtained impedance responses of FeCrAl-ODS

To evaluate the impedance more precisely, equivalent circuit analyses of the obtained impedances were performed [3], as shown in Fig. 6. A simple RC circuit was used to fit the measured impedance. The obtained time-dependent polarization resistances are shown in Fig. 7. The polarization resistance of FeCrAl-ODS at DO = 8 ppm increased rapidly and then reached a constant value after approximately 150 h, which was indicative of stabilized FeCrAl-ODS surface conditions. The polarization resistance obtained at a DO of 0.25 ppm reached a constant value in less than 50 h, which was less than that associated with a DO of 8 ppm. The polarization resistance in deaerated conditions was small just after immersion of the specimens, and then continuously increased up to 500 h, which indicated that FeCrAl-ODS corrosion occurred initially and then was suppressed by the formation of the oxide film at the surface of the FeCrAl-ODS.

The corrosion depth of FeCrAl-ODS at different DO concentrations was estimated by using the obtained polarization resistance [1]. The reciprocal of the polarization resistance was proportional to the corrosion current at the surface of FeCrAl-ODS, which determined the corrosion rate of FeCrAl-ODS according to Eq. (1).

$$I_{corr} = \frac{B}{R_p}, \qquad (1)$$

where I_{corr} is the corrosion current, B is a constant, and R_p is the polarization resistance, as determined by EIS. Unfortunately, the value of B at high temperatures was not reported. Therefore, B was taken as 0.026 in this study, which is a typical value for the corrosion of metals at room temperature [1,4]. The corrosion depth was determined using the time-dependent corrosion current, and the results are shown in Fig.8. The estimated corrosion depth of FeCrAl-ODS in deaerated conditions was the largest, but less than 3 μm.

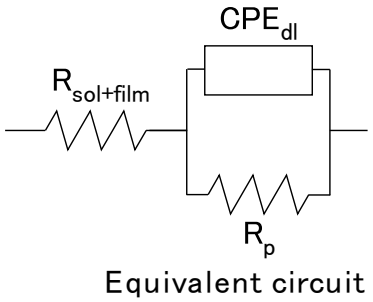

Equivalent circuit

$R_{sol+Film}$: sum of the solution resistance and film resistance
R_p: polarization resistance
C_{dl}: double layer capacitance
CPE: Constant phase element

$$Z_{CPE} = \frac{1}{(j\omega)^p T} \quad T = C_{dl}\ (\text{assumed})$$

Fig. 6 Equivalent circuit

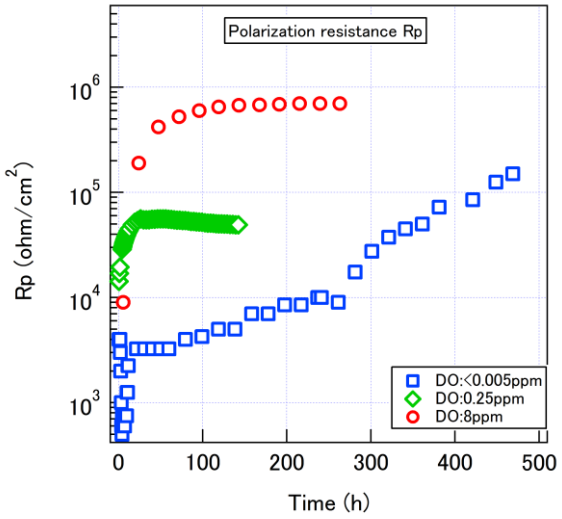

Fig. 7 Time-dependent polarization resistances

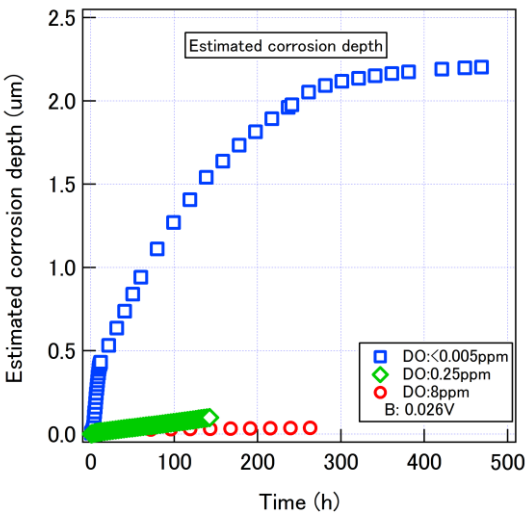

Fig. 8 Estimated corrosion depth

The SEM images of the FeCrAl-ODS after immersion are shown in Fig.9. The formation of the oxide particles was observed in all specimens. The size of particles changed with changes in the DO concentration. The size of particles at a DO of 8 ppm was smallest and the largest at a DO of 0.25 ppm. In the deaerated conditions, large and small particles coexisted.

The oxide particles at the surface of the specimens were generated by the precipitation of the dissolved iron ions. The dissolution of iron was mitigated by the oxide film that was formed on the surface, which suppressed the iron dissolution. The dissolution rate of iron at a DO of 8 ppm could be smaller than that at a DO of 0.25 ppm according to the results of EIS. Under 8 ppm DO conditions, the protective oxide film might be formed at the initial stage of the immersion. The protective oxide film under 8 ppm DO conditions might cause the formation of the smaller particles due to the suppression of the iron dissolution. In deaerated conditions, the dissolution rate was initially high and then slowed due to the formation and growth of the protective oxide film. As a result, the large particles that might get formed at the initial stage of immersion and smaller particle that might get formed after the protective film covered the surface.

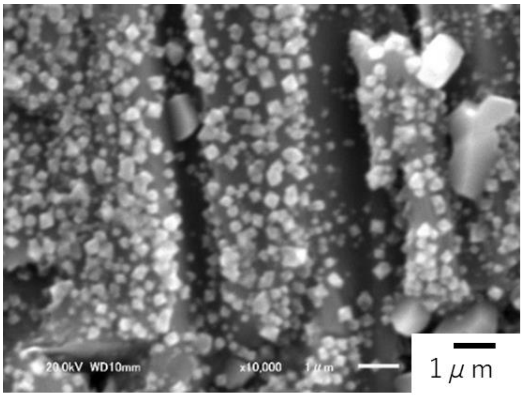

(a) <0.005 ppm

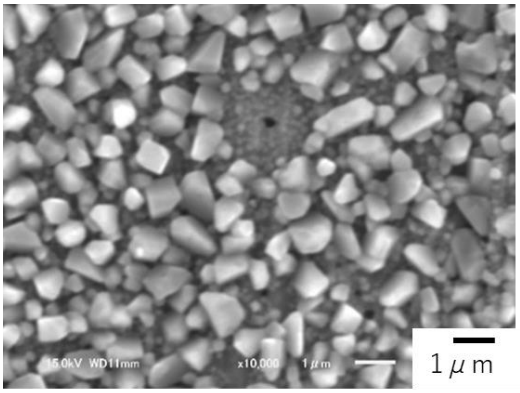

(b) 0.25 ppm

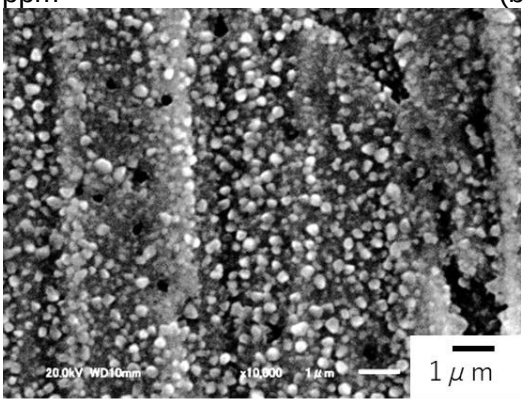

(c) 8ppm

Fig. 9 SEM images of FeCrAl-ODS after immersion test

To evaluate the content of major elements at the surface of FeCrAl-ODS, quantitative analyses of the content were performed by EDS. The analyses were performed with 3,000 magnifications. The resulting average value for the 43 x 32 μm region is listed in Table 2. The oxygen content at the surface in deaerated conditions was highest, while it was lowest under 8 ppm DO conditions. This result indicated that the largest amount of oxide formation at the surface of FeCrAl-ODS occurred in deaerated conditions, and oxide formation was the lowest under 8 ppm DO conditions. This result agreed with the dependency of the corrosion depth on dissolved oxygen concentrations obtained by EIS. To evaluate the effects of DO on the oxide film, cross-sectional observation is effective. However, the roughness of the test specimens which were mechanical polished might be much larger than the thickness of oxide film. The cross-sectional observation of oxide film using mirror surface polished specimens is a subject for further study.

	C	O	Al	Fe	Cr	Y
<0.005ppm	2.19	28.62	3.91	44.90	17.74	0.84
0.25ppm	1.81	17.22	2.34	64.78	12.21	0.39
8ppm	2.16	8.41	3.86	71.90	12.66	0.23

Table 2 Results of EDS (w%)

3.2 Effects of ion irradiation

To investigate the effects of irradiation on the corrosion of FeCrAl-ODS in high temperature water, EIS of the irradiated FeCrAl-ODS was employed. The oxygen concentrations were 8 and 0.25 ppm in this study and the time of immersion was 200 h. The Nyquist plots of the experimentally-obtained impedance responses and the Bode plots of the modulus of impedance are presented in Figs. 10 and 11 for 8 and 0.25 ppm, respectively. A clear difference in the impedance responses was not obtained between the irradiated FeCrAl-ODS specimen and non-irradiated specimen.

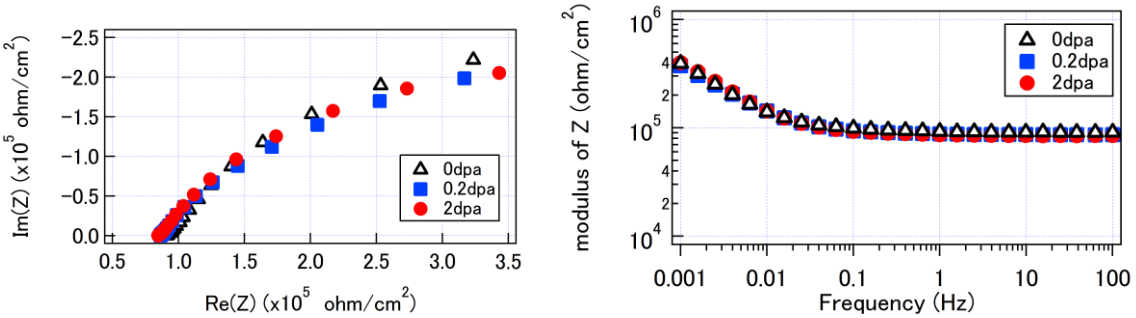

(a) Nyquist plots (b)Bode plots (modulus of Z)

Fig. 10 Impedance responses of irradiated FeCrAl-ODS (8 ppm)

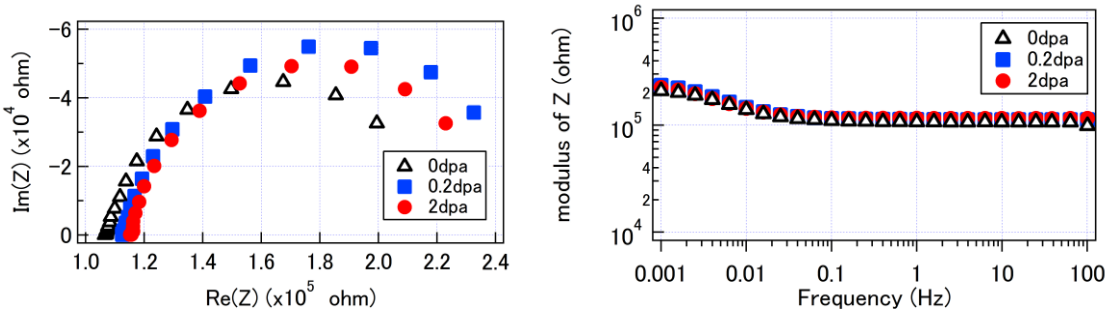

(a) Nyquist plots (b)Bode plots (modulus of Z)

Fig. 11 Impedance responses of irradiated FeCrAl-ODS (0.25 ppm)

The SEM images are shown in Figs. 12 and 13. A clear difference in the surface conditions was not observed, which indicated that the radiation damage to FeCrAl-ODS might not affect the corrosion properties of FeCrAl-ODS in high-temperature water.

The surface of specimens used in this study was relatively rough, and polishing traces were observed in SEM images for 8 ppm DO conditions. The degree of roughness might affect the corrosion associated with irradiation and using mirror surface polished specimens to evaluate the effects of roughness is a subject for further study.

The examinations performed in this study were all post-irradiation. On the contrary, the fuel cladding will be corroded under irradiation condition. Under irradiation condition, there was some indication that the oxide film, which offers some protection against corrosion, could be changed. Evaluation the change in the protection associated with the formation of the oxide film under direct irradiation is also for further study.

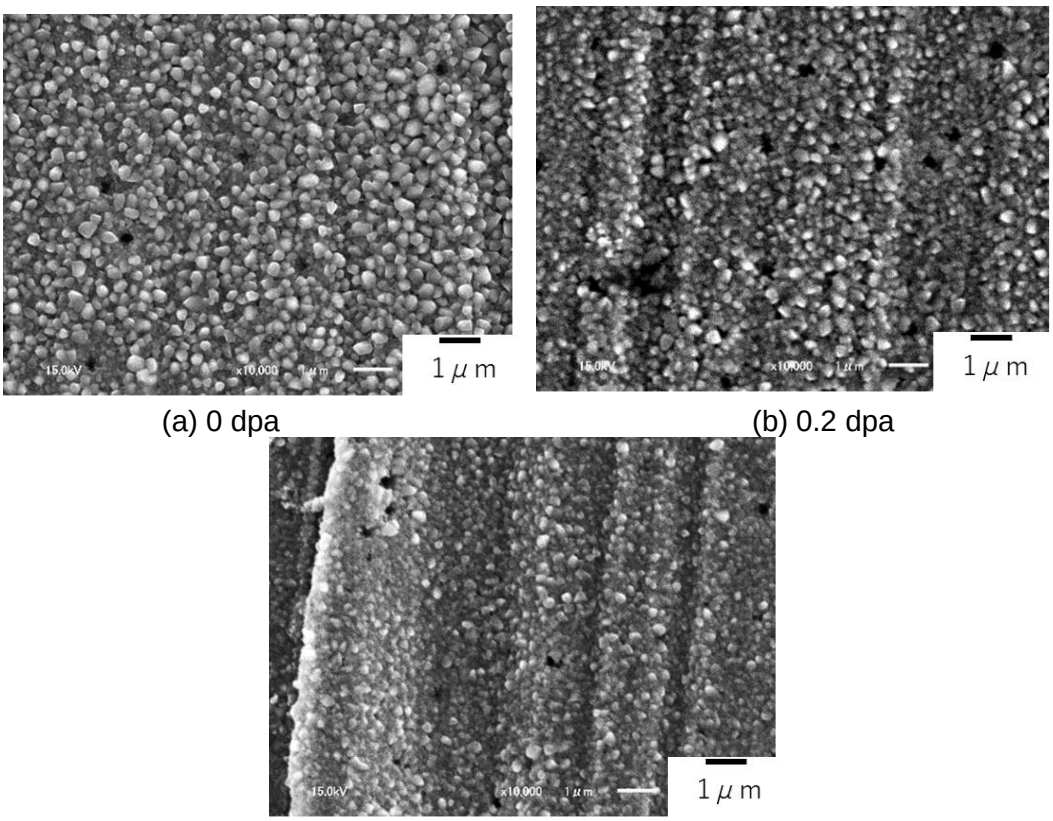

(a) 0 dpa (b) 0.2 dpa

(c) 2 dpa

Fig. 12 SEM images of irradiated FeCrAl-ODS (8 ppm, x10,000 magnification)

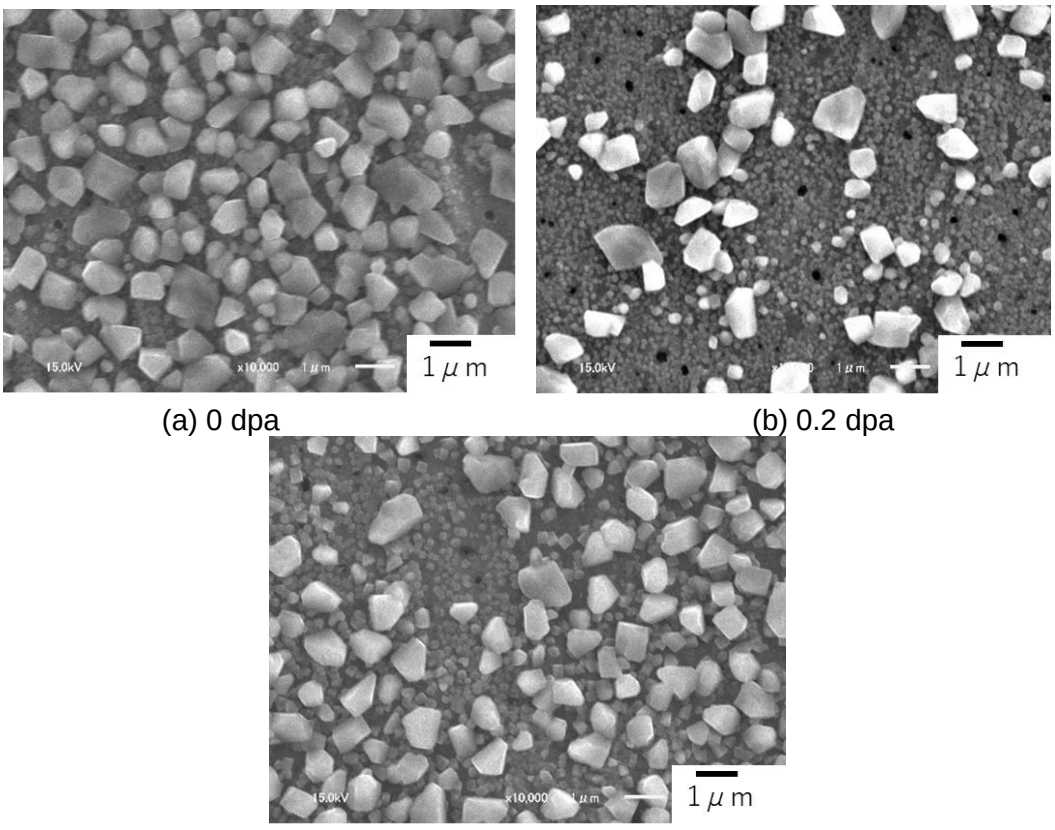

(a) 0 dpa (b) 0.2 dpa

(c) 2 dpa

Fig. 13 SEM images of irradiated FeCrAl-ODS(0.25 ppm, x10,000 magnification)

4. Conclusion

The major conclusions drawn from this study are as follows:

(1) The experimentally-obtained modulus of impedance increased with time and then reached a saturated value. The smaller the DO concentration, the longer it took to reach saturation.

(2) The estimated corrosion depth of FeCrAl-ODS under deaerated conditions was the highest, though it was less than 3 μm.

(3) The modulus of the impedance responses of the irradiated FeCrAl-ODS specimen was virtually the same as that of the non-irradiated specimen, which indicated that the radiation damage to FeCrAl-ODS might not affect the corrosion properties of FeCrAl-ODS in high-temperature water.

5. References

[1] T.Satoh, Y.Yamamoto, T. Tsukada, C.Kato, "*In-situ* Measurement of Corrosion Environment in High Temperature Water without Electrolyte Utilizing Electrochemical Impedance Spectroscopy"Zairyo-to-Kankyo,64, 91-97, (2015)(in Japanese)

[2] T.Satoh, S.Uchida, J.Sugama, N.Yamashiro, T.Hirose, Y.Morishima, Y.Satoh and K.Iinuma, "Effects of Hydrogen Peroxide on Corrosion of Stainless Steel, (I)", Journal of Nuclear Science and Technology, 41, 610 (2004)

[3] M.E.Orazem and B. Tribollet "Electrochemical Impedance Spectroscopy", John Wiley & Sons, Inc. (2008)

[4] M. Stern, E.D.Weisert, "Experimental observations on the relation between polarization resistance and corrosion rate", Proc. ASTM, 59, 1280 (1959)

Acknowledgment

This study is the result of "Development of Technical Basis for Introducing Advanced Fuels Contributing to Safety Improvement of Current Light Water Reactors" carried out under the Project on Development of Technical Basis for Improving Nuclear Safety by Ministry of Economy, Trade and Industry (METI) of Japan.